Sixth International Symposium on Turbulence and Shear Flow Phenomena
Seoul, Korea, 22-24 June 2009

USING LES TO MODEL TURBULENT PARTICLE TRANSPORT IN HUMAN LUNGS

H. Radhakrishnan and S. Kassinos
Department of Mechanical and Manufacturing Engineering
University of Cyprus
Nicosia, Cyprus
hariradh@ucy.ac.cy

ABSTRACT

Understanding transport and deposition of inhaled particles in the human airways plays a crucial role in the targeted therapy of pulmonary diseases, and the administration of inhaled medicines. Numerous researchers have studied the inhalation of particles using experiments or computer models. Even though experiments have shown that the airflow in the trachea and the upper branches of the lung is turbulent, the flow is taken to be laminar in most computer models. Only few recently published papers have looked at the turbulent transport of air in the human airways. Even fewer results have been published on the effect of the upper airway structures on the turbulent airflow in the lungs or on the effect of the turbulence on particle deposition. The previously published turbulent models have also mainly used RANS methods to predict the flow. To study the unsteady flow and particle deposition in a human lung, an LES model with a dynamic Smagorinsky sub-grid scale model was used. The model equations were solved to study steady inspirational flow at different flow rates for different particle sizes. Results indicate that the upper airway geometry produces turbulence in the flow and the deposition of particles is mainly affected by the particle size and Stokes number.

INTRODUCTION

Solid particles like pollen, dust, and particulate pollutants, and liquid particles like aerosolized fuel are present in the air everywhere. These particles are constantly inhaled and deposited in the airways. Some medicines like corticosteroids used to control asthma are also nebulized and administered as inhaled particles. Thus, understanding the transport and deposition of inhaled particles in the human airways plays a crucial role in the administration of such medicines Usmani *et al.* (2003), and in the development of diseases caused by inhaled particles (Balásházy *et al.* 2003, Schlesinger & Lippmann 1978). Research by Usmani *et al.* (2003) has shown that only 10 to 20% of the inhaled drug reaches the lungs. Experimental studies by Schlesinger & Lippmann (1978) using casts of the human airways show a high correlation between regions of high particle deposition and primary origin sites of bronchial carcinoma. Therefore, it is crucial to understand the factors that affect particle deposition in the lungs in order to improve drug delivery mechanisms for targeted therapy of pulmonary diseases. It is an interesting field of current research and numerous researchers have investigated the inhalation of particles in the human airways using experiments or numerical simulations.

Cheng *et al.* (1999) studied flow and particle deposition in casts of human airways; Caro *et al.* (2002) created ideal models of the human lungs for their experiments. In both cases, experiments revealed that the airflow in the trachea and upper bronchi is turbulent. Most computer models, for example Liu *et al.* (2002) and Comer *et al.* (2001a,b), have so far assumed the airflow to be laminar. To justify this assumption, the analysis is restricted to the branches below the third generation where the flow is laminar because of their small diameters (Comer *et al.* 2001a,b). A few recent papers have looked at turbulent transport of air and particles in the human airways but have primarily employed RANS models.

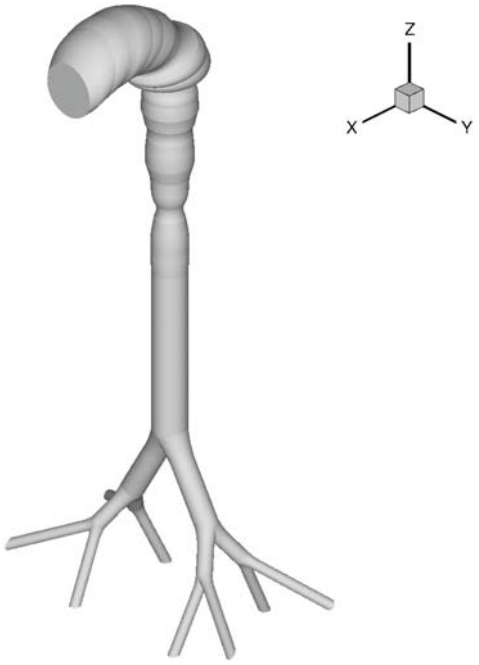

Figure 1: Model of the human mouth, throat, and airways used to study particle deposition.

Zhang & Kleinstreuer (2004) used the k-ω RANS model to study turbulent airflow and particle deposition in the airways. The k-ω model have also been used by other researchers to model airflow in the lungs. Recently, Calay *et al.* (2002) and Luo *et al.* (2004) have used LES to study turbulent flow and particle deposition in the lungs, but they did not consider the effect of the upper airway features. Lin *et al.* (2007) have recently used DNS to study steady inspirational flow in the airways but they did not consider particle deposition in the airways. In the work reported here, LES is used to study turbulent flow and particle deposition in the upper airways and lungs.

METHOD

The lung was modeled using two sources. The upper air-

way geometry was modeled using the cross-sectional areas of the human thorax reported by Cheng *et al.* (1999). The cross-sectional areas were recast as diameters which were used to model the geometry of the oral cavity and the upper airway up to the trachea. The trachea and the branches were modeled as a symmetrically bifurcating series of pipes based on the regular dichotomy model of Weibel (1963). The axis of the daughter branches were offset by 30° from the axis of the originating branch, and the plane of each branch level was rotated from the plane of the previous level by 90°. The last level of branches were terminated in to a common reservoir used to represent the lower bronchi, alveoli, and other structures in the lung not considered in the model. The solutions in this reservoir are ignored during the analysis of results. The final geometry used in the LES computations is shown in Figure 1. The geometry was meshed using approximately three million control volumes. The resolution of the mesh was verified by comparing the LES solutions with solutions computed on the same mesh without using a sub-grid scale model. The maximum difference in the turbulent kinetic energy estimates was less than 7 % indicating the mesh was fine enough for well-resolved LES.

The flow of air in the lungs, assumed to be incompressible, is described by the Navier-Stokes equation and the mass continuity equation:

$$\frac{\partial \mathbf{v}}{\partial t} + \mathbf{v} \cdot \nabla \mathbf{v} = -\frac{1}{\rho}\nabla p + \mathbf{g} + \nu \nabla \cdot (\nabla \mathbf{v} + \nabla \mathbf{v}^T) \quad (1)$$

$$\nabla \cdot \mathbf{v} = 0 \quad (2)$$

where $\mathbf{v}$ is the air velocity, p is the local pressure, ρ is the density of air, taken to be 1.2 kg/m^3, and ν is the kinematic viscosity of air taken to be 1.5×10^{-5}m^2/s. A finite-volume solver based on LES with a dynamic Smagorinsky sub-grid scale (SGS) model is used to solve the model equations in the lung geometry to study steady inspirational flow at flow rates of 30 l/min and 60 l/min for particles with diameters of 1 μm, 5 μm, and 10 μm. The dynamic Smagorinsky SGS model was chosen because it does not fail even when the flow becomes transitional or laminar. This is very critical in the study of flow in the lungs where the flow transitions from laminar to turbulent not only in time with inhalation and exhalation but also in space as the bronchi become smaller at the lower levels.

At the mouth, a uniform velocity profile was used as the inlet boundary condition. A parabolic profile, and fully developed turbulent flow profiles were also tried but the results in the trachea did not show any significant difference. Hence, the uniform profile was used because it was the easiest to implement. At the outlet of the reservoir, a penalty boundary condition is applied to ensure that the net mass within the geometry is conserved. The incompressibility condition is enforced using a pressure-Poisson equation.

Coupling between the flow and the particles is one-way, i.e. the particles are aware of the flow and are affected by the flow but the flow is not affected by the presence of the particles. The particles are modeled as point particles. The solutions of the LES model for the volumetric flow rate of 60 l/min and 1 μm, 5 μm, and 10 μm diameter particles are reported below.

RESULTS AND DISCUSSION

Computational results showed that the constrictions, expansions, and other structures in the upper airway produced turbulence in the airflow in the lungs. Eddies and structures produced in the upper airway are carried into the lower branches of the lungs. Figure 2 shows the isobars at different locations in the oral, pharyngeal, and tracheal regions. Comparing the pressure contours at locations B, the epiglottis, and C, the glottal region, in Figure 2 shows that the average pressure near the walls at the glottis (C) are higher that the pressure near the walls at the epiglottis (B). The almost concentric contours at the epiglottis (B), glottis (C), and the larynx (D) indicate that there are strong jets oriented along the axial direction. The jet at the glottis (C) is biased dorsally, i.e. towards the back, as indicated by the off-centered contours. The jets have almost dissipated by the time the flow reaches the trachea (E). The flow starts to split into two as it approaches the first bifurcation. Figure 3 shows the average pressure contours near the first bifurcation. The location marked A is the same location as the one marked F in Figure 2. Comparing the pressures at B, and C and D in the two branches indicates that the flow splits nearly symmetrically.

Figure 4 shows the contours of the velocity along the tracheal axis, which is the z-axis, as seen in Figure 1. Most of the reported values are negative because the flow is down the z-axis. Positive values seen immediately downstream of the epiglottis (B), combined with the adverse pressure gradient seen between the epiglottis (B) and the glottis (C) in Figure 2 indicate the presence of reverse flow and recirculation. The highest velocity is seen at the larynx (D) which is the narrowest part of the airway. Recirculation regions and separated flow can be seen immediately downstream of the larynx in Figure 4. The turbulence characteristics of the flow can be better understood by looking at the kinetic energy distribution in the flow.

The mean kinetic energy (MKE) of the flow is defined as $\sqrt{\bar{u}^2 + \bar{v}^2 + \bar{w}^2}$ where $\bar{u}$, $\bar{v}$, and $\bar{w}$ are the time-averaged cartesian velocity components. The turbulent kinetic energy (TKE) of the flow is defined as $\sqrt{u'^2 + v'^2 + w'^2}$ where u', v', and w' are the root mean square velocity components along the three cartesian directions. The MKE and TKE of the flow in the upper airway are plotted in Figure 5. Regions with high MKE in Figure 5(a) are the regions with the fastest flow, in this case, the epiglottis (B) and larynx (D) shown in Figure 2. In Figure 5(a), regions with low MKE close to the bronchi walls near the bifurcation point indicate that the flow is separating from the walls there. A stagnation point is also visible at the ridge of the bifurcation point, as indicated by the low MKE there. Figure 5(b) plots the turbulent kinetic energy of the flow. Regions with high TKE are regions where the velocity is fluctuating rapidly, and the turbulence is the highest. The regions with the highest TKE are the regions immediately downstream of the epiglottis (B) and the larynx (D) which also show reverse flow in Figure 4.

Figure 6(a) shows the iso-surface where the average velocity magnitude is 37.5% of the maximum, and Figure 6(b) shows the iso-surface where the average velocity magnitude is 25% of the maximum. The iso-surface in Figure 6(a) shows the tracheal jet which starts at the larynx and breaks up as it nears the first bifurcation. This jet was also reported in the DNS results of Lin *et al.* (2007). The iso-surface in Figure 6(b)f shows the jet that starts from the epiglottis and then strikes the dorsal wall of the glottis. This epiglottal jet was seen in the experimental results of Kim *et al.* (1994). This jet can also be seen in the MKE distribution in Figure 5(a).

The distribution of 1 μm, 5 μm, and 10 μm diameter particles in the mouth and throat are shown in Figure 7. The 1 μm particles which have the least inertia are sensitive to even the smallest scales of turbulence and are distributed

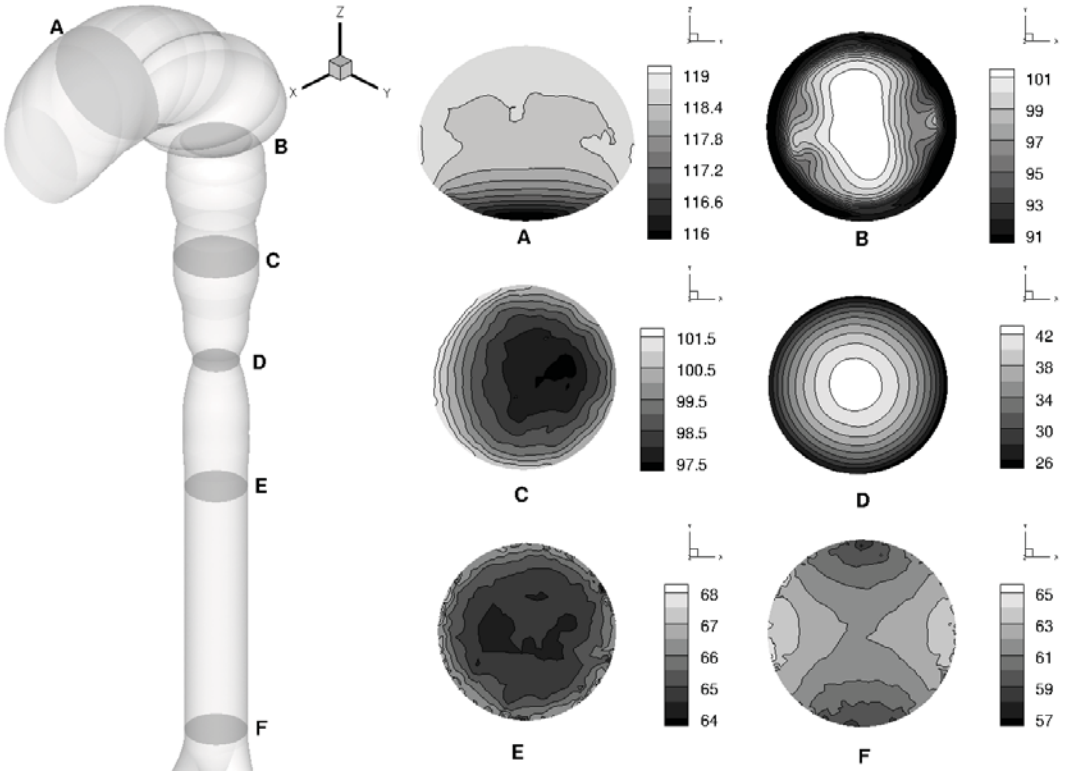

Figure 2: Pressure contours at different locations in the mouth and throat region.

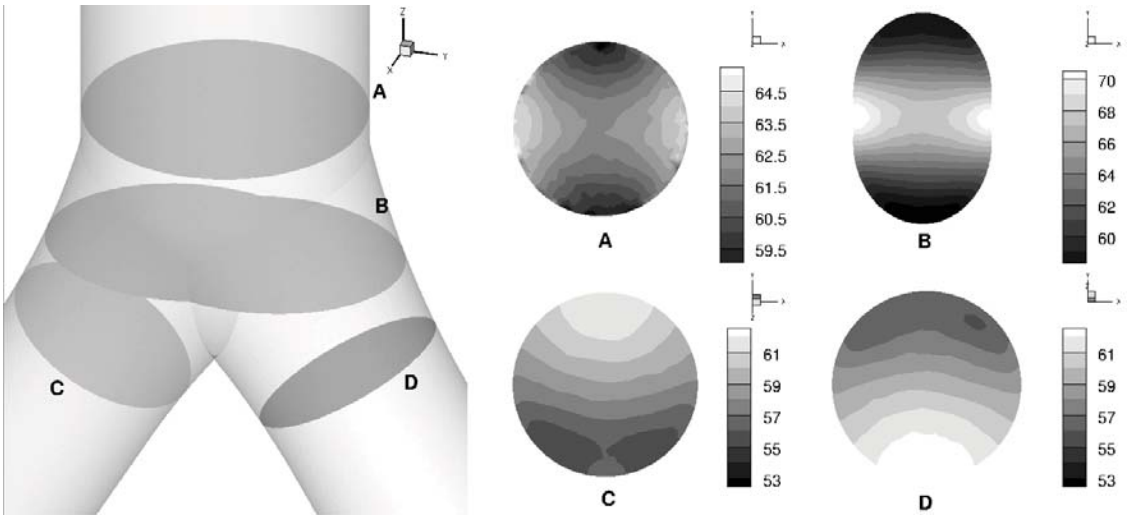

Figure 3: Pressure contours at different locations in the trachea and first branches.

almost uniformly. The 10 μm particles have the most inertia and tend to follow the mean flow. The 10 μm particles are seen to be concentrated close to the dorsal wall of the glottis because of the epiglottal jet seen in Figure 6(b).

Figure 8 shows the deposition pattern of the 1 μm, 5 μm, and 10 μm diameter particles at the first three bifurcation levels. Because most deposition occurs by inertial impaction, the particles are concentrated near the bifurcations. Larger quantities of the bigger particles are deposited compared to the smaller particles, which is also observed in experimental and other numerical results. Most of the smaller particles are swept in to the lower levels of the lungs where they get deposited. A small number of particles are trapped in the recirculation downstream of the larynx, and deposited on the tracheal wall close to the larynx. More 1 μm particles are deposited relative to 5 μm and 10 μm particles because the larger particles are not very sensitive to the secondary flows.

CONCLUSIONS AND FUTURE WORK

A finite volume solver using an LES model with dynamic Smagorinksy SGS was used to study turbulent airflow and particle deposition in the human lungs. Results show that structures in the upper airway geometry trigger turbulence in the flow, and this turbulence affects the particle distribution and deposition. The distribution and deposition patterns are strongly dependent on the particle size and Stokes number.

The present work was restricted to steady inspirational

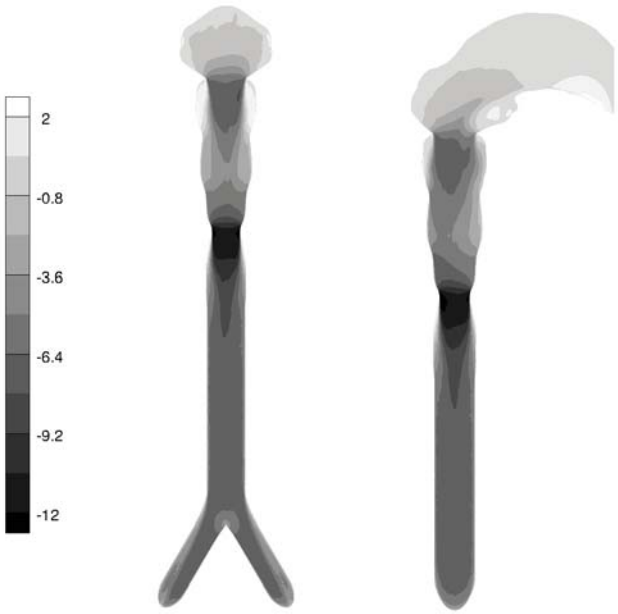

Figure 4: Isopleths of time-averaged velocity in the oral, pharyngeal, and tracheal regions along the tracheal axis.

flow, and its effects on particle deposition. It is being expanded to study the effect of cyclical flow on particle deposition and the differences between flow and deposition in adult and juvenile airways, and healthy and diseased airways.

ACKNOWLEDGMENTS

The research described in this paper has been performed under the UCY-CompSci project, a Marie Curie Transfer of Knowledge (TOK-DEV) grant (Contract No. MTKD-CT-2004-014199), funded by the CEC under the 6th Framework Program. It was also partly supported by a Center of Excellence grant from the Norwegian Research Council to Center for Biomedical Computing.

REFERENCES

Balásházy, Imre, Hofmann, Werner, & Heistracher, Thomas. 2003. Local particle deposition patterns may play a key role in the development of lung cancer. *Journal of Applied Physiology*, **94**, 1719–1725.

Calay, R K, Kurujareon, Jutarat, & Holdo, Arne Erik. 2002. Numerical simulation of respiratory flow patterns within human lung. *Respir Physiol Neurobiol*, **130**(2), 201–221.

Caro, C. G., Schroter, R. C., Watkins, N., Sherwin, S. J., & Sauret, V. 2002. Steady inspiratory flow in planar and non-planar models of human bronchial airways. *Proc. R. Soc. Lond. A*, **458**, 791–809.

Cheng, Yung-Sung, Zhou, Yue, & Chen, Bean T. 1999. Particle Deposition in a Cast of Human Oral Airways. *Aerosol Science and Technology*, **31**, 286–300.

Comer, J. K., Kleinstreuer, C., & Zhang, Z. 2001a. Flow structures and particle deposition patterns in double-bifurcation airway models. Part 1. Air flow fields. *J. Fluid Mech.*, **435**, 25–54.

Comer, J. K., Kleinstreuer, C., & Zhang, Z. 2001b. Flow structures and particle deposition patterns in double-bifurcation airway models. Part 2. Aerosol transport and deposition. *J. Fluid Mech.*, **435**, 55–80.

Kim, Chong S., Fisher, Donald M., Lutz, David J., & Gerrity, Timothy R. 1994. Particle Deposition in Bifurcating Airway Models With Varying Airway Geometry. *J. Aerosol Sci.*, **25**(3), 567–581.

Lin, Ching-Long, Tawhai, Merryn H., McLennan, Geoffrey, & Hoffman, Eric A. 2007. Characteristics of the turbulent laryngeal jet and its effect on airflow in the human intra-thoracic airways. *Respiratory Physiology & Neurobiology*, **157**(2-3), 295–309.

Liu, Y., So, R. M. C., & Zhang, C. H. 2002. Modeling the bifurcating flow in a human lung airway. *Journal of Biomechanics*, **35**, 465–473.

Luo, X Y, Hinton, J S, Liew, T T, & Tan, K K. 2004. LES modelling of flow in a simple airway model. *Medical Engineering & Physics*, **26**(5), 403–413.

Schlesinger, Richard B., & Lippmann, Morton. 1978. Selective particle deposition and bronchogenic carcinoma. *Environmental Research*, **15**(June), 424–431.

Usmani, Omar S., Biddiscombe, Martyn F., Nightingale, Julia A., Underwood, S. Richard, & Barnes, Peter J. 2003. Effects of bronchodilator particle size in asthmatic patients using monodisperse aerosols. *J. Appl. Physiol.*, **95**, 2106–2112.

Weibel, Ewald R. 1963. *Morphometry of the human lung.* Berlin: Springer-Verlag.

Zhang, Z., & Kleinstreuer, C. 2004. Airflow structures and nano-particle deposition in a human upper airway model. *Journal of Computational Physics*, **198**, 178–210.

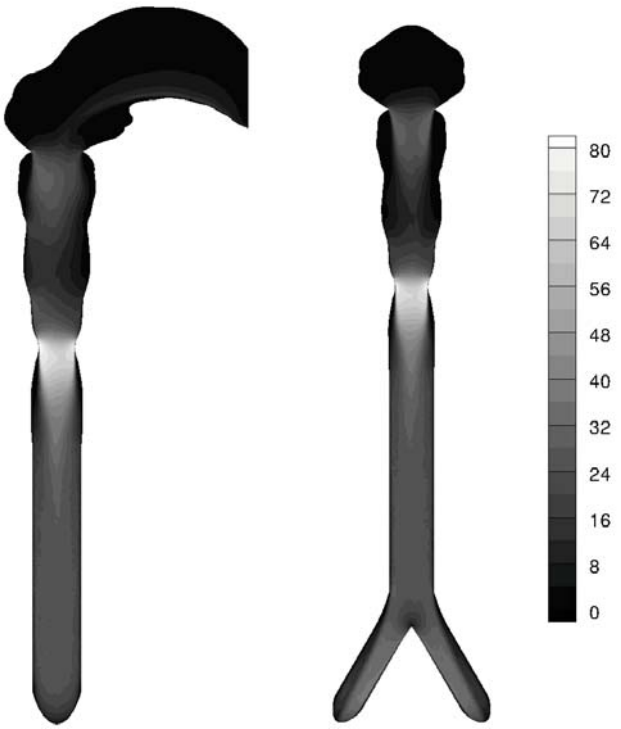

(a) Mean kinetic energy distribution

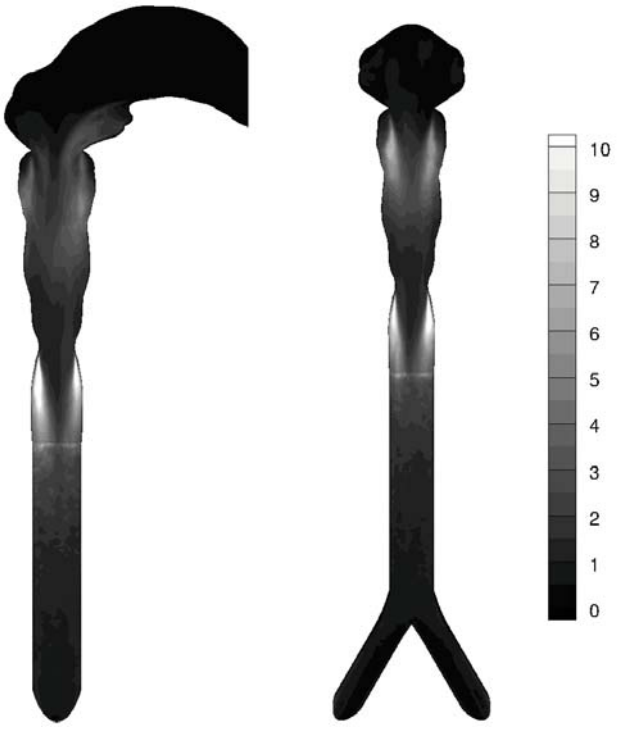

(b) Turbulent kinetic energy distribution

Figure 5: Distribution of kinetic energy in the upper parts of the human airways.

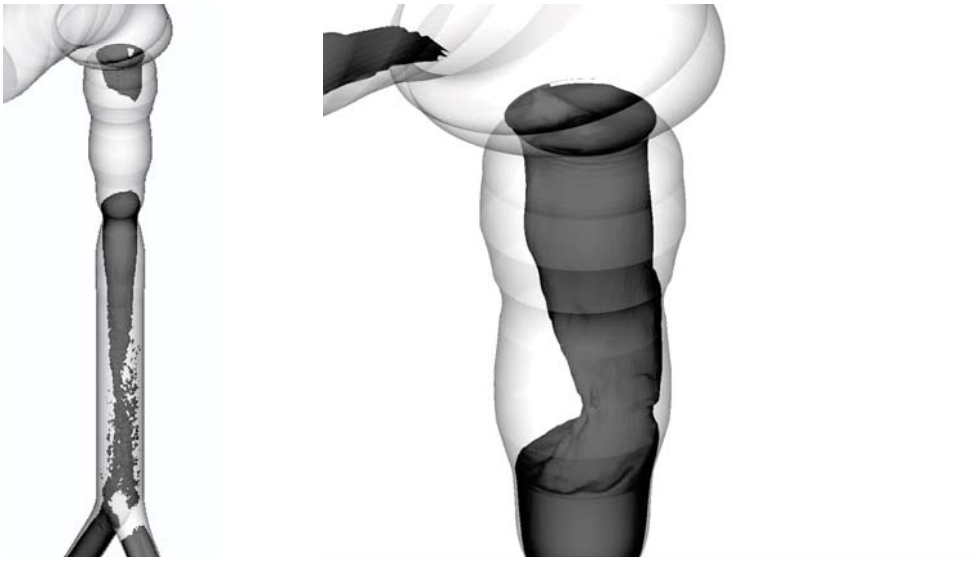

(a) 1 μm particles (b) 5 μm particles

Figure 6: Jets arising from the epiglottis and larynx are seen by plotting iso-surfaces of mean velocity magnitude.

(a) 1 μm particles (b) 5 μm particles (c) 10 μm particles

Figure 7: Distribution of particles in the mouth and throat.

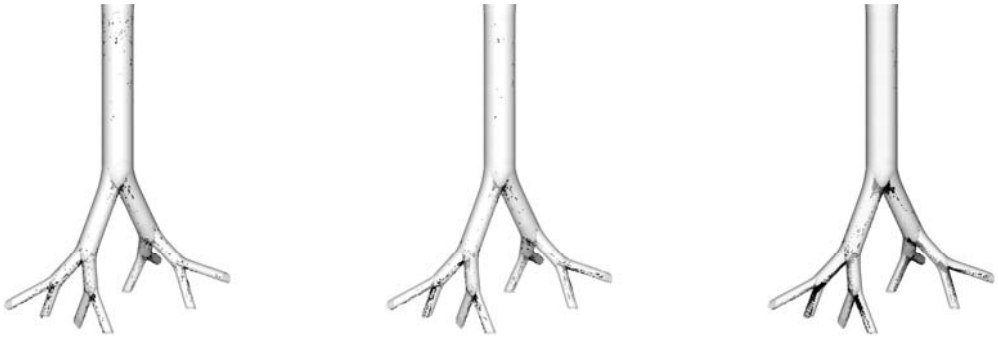

(a) 1 μm particles (b) 5 μm particles (c) 10 μm particles

Figure 8: Distribution of deposited particles in the branches of the lung.